

# Connecting Experimental and Modeling Uncertainties Using Fission Observables

Fanta Diaby<sup>1,\*</sup>, Denise Neudecker<sup>1</sup>, and Amy E. Lovell<sup>1</sup>

<sup>1</sup>Los Alamos National Laboratory, Los Alamos, NM, 87545, USA

**Abstract.** Understanding fission processes presents a challenge due to their complex nature. Our study begins with a comprehensive assessment of the uncertainty of experimental fission cross-section data for  $^{235}\text{U}$  using the template of expected fission cross-section measurement uncertainties to identify missing uncertainties. The code ARIADNE, developed at Los Alamos National Laboratory (LANL), is employed to quantify these experimental uncertainties. This work presents progress towards connecting pre- and post-scission fission modeling with experimental uncertainty quantification for fission cross sections. To this end, the study uses two theoretical model codes developed at LANL: CoH for modeling  $^{239}\text{Pu}$  fission cross section and the fission event generator CGMF for computing prompt fission observables. The multi-chance fission probability (MCFP) derived from sampling the fission barrier parameters in CoH covering the range of experimental data is utilized as input to CGMF, and its impact on the average prompt fission neutron multiplicity ( $\bar{\nu}$ ) is examined. The 20% spread in the multi-chance fission probabilities corresponds to a negligible spread in  $\bar{\nu}$  of approximately 0.5% at the second- and third-chance fission thresholds.

## 1 Introduction

The process of fission is to date an active field of study. The fission cross section, which is important in numerous nuclear applications, also presents its own set of challenges. Even with well-known isotopes like  $^{239}\text{Pu}$  and  $^{235}\text{U}$ , uncertainties in their experimental data must be considered to provide realistic evaluated mean values and to provide a realistic cross section for model fitting. The significant variations in the calculated fission cross section due to changing model parameters within physical bounds emphasize the need for experimental data to improve accuracy in modeling.

For this paper, we re-estimated experimental uncertainties for selected  $^{235}\text{U}$  fission cross section experimental data in the Neutron Data Standards database [1] (see Section 2). This database encompasses data that were judged as adequate for evaluations by the standards community and yields the evaluated standards cross section. However, it was shown in Ref. [2] for  $^{239}\text{Pu}$  fission cross sections that important uncertainty sources were missing for many of the experiments. The need to address these uncertainties has led to the development of a template of expected measurement uncertainties by the CSEWG (Cross Section Evaluation Working Group) covariance team and the Nuclear Data Standard committee [4]. This work expands on that of Section Ref. [2] by identifying and quantifying missing uncertainties of  $^{235}\text{U}$  fission cross sections via the ARIADNE code [3] and the template of expected measurement uncertainties [4]. The provided template has been systematically applied to all the  $^{239}\text{Pu}$  experimental data at

LANL [2], in collaboration with the IAEA Neutron Data Standards committee. For this work, this approach has also been extended to encompass the  $^{235}\text{U}$  cross-section data within the framework of the Neutron Data Standard.

In section 3, we link the fission cross section to prompt fission observables. Specifically, we aim to connect the fission cross section (pre-scission) in CoH [5] to prompt fission (shortly after scission) observables in CGMF [6] through the multi-chance fission probabilities (MCFPs).

## 2 Experimental Uncertainty Quantification

We start by performing a detailed uncertainty quantification of the neutron induced fission cross-section experimental data. This uncertainty estimate is undertaken with the help of the code ARIADNE [3]. This code is a LANL Python program created to assist evaluators in efficiently estimating detailed uncertainties and correlations in experimental data.

### 2.1 Measurement Features

The fission cross-section experimental data are retrieved from the GMA [1] and EXFOR [7] databases, which are databases containing updated lists of experimental reaction data. We also collect, for each dataset, various measurement features, such as the techniques and equipment used in the experiments. For example, these features may contain details about the detectors used to collect the experimental fission cross-section data. Some of these features may be linked to unidentified sources of bias. These

\*e-mail: fdiaby@lanl.gov

features allow us to undertake machine learning studies that link specific measurement feature biases in the data [8]. Such studies can guide experts in identifying drivers of bias in experimental databases and either correcting data, increasing uncertainties or rejecting them, which should ultimately lead to a better understanding of the fission cross section and more reliable evaluated uncertainties.

## 2.2 Template of Expected Measurements Uncertainties

Here, we identify first the various missing sources of uncertainties for data sets in Table 1 and then use the template of expected measurement uncertainties for fission cross section to estimate any missing uncertainties in measurement. This template is designed to help quantify the uncertainty in experimental data when a particular source of uncertainty has not been considered, providing a more robust estimate of the uncertainties in the expected measurements.

## 2.3 UQ Analysis in ARIADNE

Figure 1 represents one set of experimental data for the fission cross-section of  $^{235}\text{U}$  as a function of energy. These plots are based on the Buleeva 1988  $^{235}\text{U}$  fission cross-section experiment including their respective uncertainties [9]. It can be seen that adding missing uncertainty sources via templates of expected measurement uncertainties did increase the final experimental uncertainties compared to those in the GMA database.

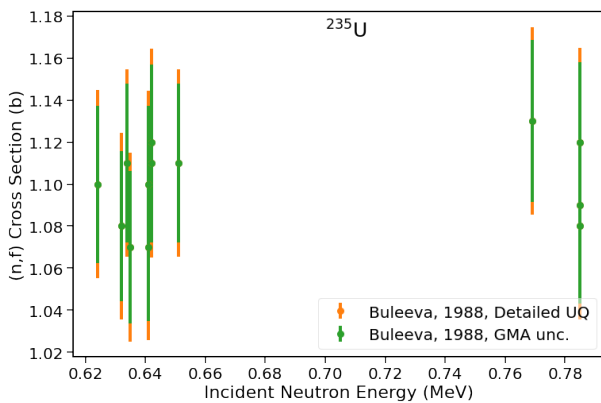


**Figure 1.** The experimental fission cross sections conducted by N. N. Buleeva et al. were obtained from GMA [1], and the uncertainties associated with the data were subsequently corrected using appropriate templates.

## 3 Connection between the fission cross section and prompt fission observables

To connect the fission cross section with prompt fission observables, the MCFPs calculated with CoH [5] are used as input for CGMF [6]. To understand the uncertainty of the MCFP, coming from the uncertainty on the fission cross

**Table 1.** The  $^{235}\text{U}$  fission cross-section experiments are listed for which a detailed uncertainty quantification was undertaken. Their updated and original GMA uncertainty range are also provided [1].

GMA#	Author	Unc.	Unc.New
1025	A.D.Carlson	1.9-2.9	1.82-3.3
1028	P.W. Lisowski	1.2-8.0	0.98-21.4
499	P.H.White	2.6-3.2	1.58-2.34
501	P.H.White	2.8-3.8	2.07-3.67
504	I.Szabo	3.1-3.3	1.59-5.56
505	I.Szabo et al.	3.1-3.2	1.77-3.15
506	I.Szabo et al.	3.4-4.1	2.84-4.24
508	A. D. Carlson	1.6-3.2	1.82-3.1
509	A. D. Carlson	2.2-2.6	2.35-2.8
510	J.B. Czirr	1.6-6.6	1.48-3.41
511	J.B. Czirr	1.4-4.4	1.73-2.2
518	G.F.Knoll	4.7	1.46
520	K. Kari	2.9-3.7	1.56-11.09
522	N.N.Buleeva	3.3-3.4	3.94-4.19
524	A.D Carlson	1.2-2.0	0.81-3.11
525	E.A.Schagrov	3.6-3.7	1.92-2.58
526	C.A.Uttley	3.5	2.05
553	W.P. Poenitz	1.8-3.1	3.76-9.83
554	W.P.Poenitz	2.0-2.9	1.43-5.93
555	W.P.Poenitz	2.1-3.6	1.86-5.37
556	W.P. Poenitz	1.8-3.0	1.52-3.22
557	W.P.Poenitz	2.5	2.05
559	W.P. Poenitz	2.0-3.8	1.54-5.27
560	W.P.Poenitz	3.9-3.9	2.84-2.84
561	W.P.Poenitz	3.6-3.8	2.83-3.31
567	R.K.Smith	5.2-7.4	3.34-10.8
568	W.D.Allen	4.4-10.7	3.74-10.67
570	O.A.Wasson	2.2-2.6	1.81-2.07
580	D.M.Barton	1.0-2.4	1.28-3.36
582	Kaeppler	2.2-2.4	1.39-5.22
590	Tud/Kri Collab.	2.2	1.88
591	Tud/Kri Collab.	1.2	1.75
597	M.Cance	1.6-2.1	1.66-2.36
598	M.Cance	2.8-2.8	2.27-2.27
645	Li Jingwen	1.7	0.91
738	Yan Wuguang	4.6-4.7	4.89-5.19

section, on prompt fission observables, we sample the fission cross-section parameters in CoH, primarily the fission barrier heights and curvatures. Here, we primarily focus on the average prompt fission neutron multiplicity,  $\bar{\nu}$ , which is the average number of neutrons released immediately following fission.

### 3.1 Multi-chance fission probabilities from sampling the fission barrier parameters

To vary the MCFPs, we sampled both the fission barrier heights and curvatures within CoH. Both were sampled uniformly, within a range of  $\pm 2\%$  of the baseline value for the heights and  $\pm 10\%$  for the curvatures, the ranges of which are chosen based on expert judgement. The fission barriers for  $^{240}\text{Pu}$ ,  $^{239}\text{Pu}$ ,  $^{238}\text{Pu}$ , and  $^{237}\text{Pu}$  were all

sampled 100 times simultaneously in this manner, corresponding to first-, second-, third-, and fourth-chance fission. These changes ensure that the parameters remain physical and within the spread of the experimental data. The graph shown in Fig. 2 demonstrates the spread in the individual MCFPs as a function of the incident neutron energy. The black band represents the first-chance probability, which remains at 100% until around 5 MeV, after which it starts to decline due to the opening of the second-chance fission channel. The non-zero values in the second (in red), third (in blue) and fourth (in green) chances correlate with the channel being energetically accessible. The probability indicates the competition between the two fission channels.

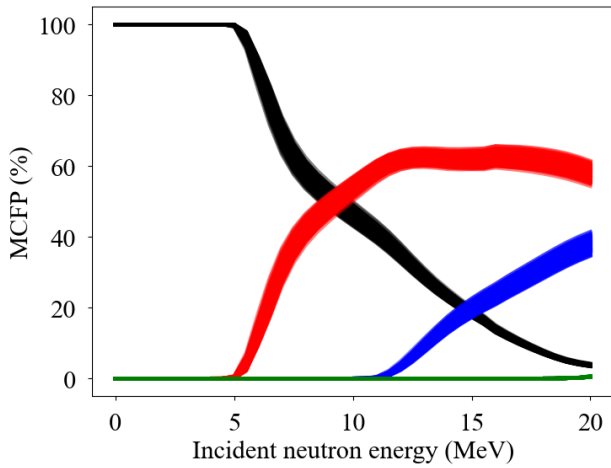


**Figure 2.** The spread in the multi-chance fission probabilities in  $^{239}\text{Pu}$  based on sampling CoH fission barrier parameters.

The relative spread in the computed MCFPs is calculated as:

$$MCFP(\%) = \left( \frac{\sigma_{max} - \sigma_{min}}{\sigma_{initial}} \right) * 100\% \quad (1)$$

where  $\sigma_{max}$  and  $\sigma_{min}$  are the maximum and minimum probabilities obtained from random sampling at each incident energy, while  $\sigma_{initial}$  represents the baseline probability. The relative spread is around 20%, indicating a significant change in the MCFP that can keep the fission cross section within physical bounds.

The graph in Fig. 3 shows the relative probability calculated in Eq. (1) as a function of incident neutron energy compared to the original calculation.

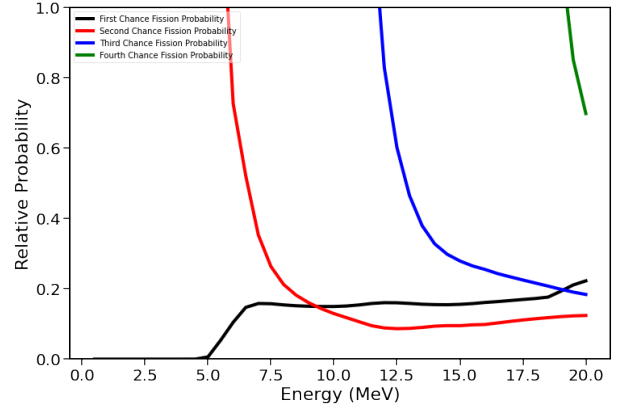


**Figure 3.** Relative spread in the MCFPs coming from the sampling of fission barrier parameters in CoH, as defined in Eq. (1).

### 3.2 Impact on prompt fission observables

The  $^{239}\text{Pu}$  MCFPs, which were calculated using CoH, are then used as input into CGMF to understand the impact on prompt fission observables. We focus here on the results for  $\bar{\nu}$ . The spread in the sampled  $\bar{\nu}$  values is shown in Fig. 4. We expect that there should be no spread in  $\bar{\nu}$  below about 5 MeV incident neutron energy, where only the  $^{240}\text{Pu}$  compound can fission (first-chance fission), but the spread appears to be negligible at all incident energies.

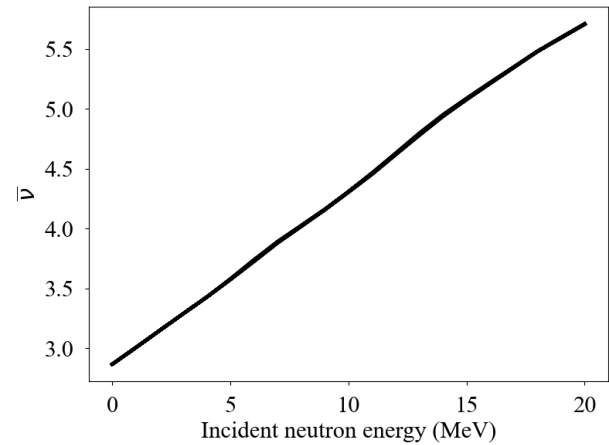


**Figure 4.** Average prompt fission neutron multiplicity,  $\bar{\nu}$ , as a function of incident neutron energy for  $^{239}\text{Pu}(n,f)$  calculated from the MCFP samples shown in Fig. 2.

To more closely investigate the spread in  $\bar{\nu}$  coming from the MCFP, we calculate the relative spread, as in Eq. (1), which is then plotted in Fig. 5. Here, we observed a relative spread of only 0.5% at the second- and third-chance fission thresholds. This spread is significantly smaller than the spread of 20% that is seen from the MCFPs themselves, indicating that, without changing other parameters, the MCFPs do not have a significant impact on  $\bar{\nu}$ . Other prompt fission observables, not shown in this work, are observed to have a slightly larger spread due to the MCFP sampling.

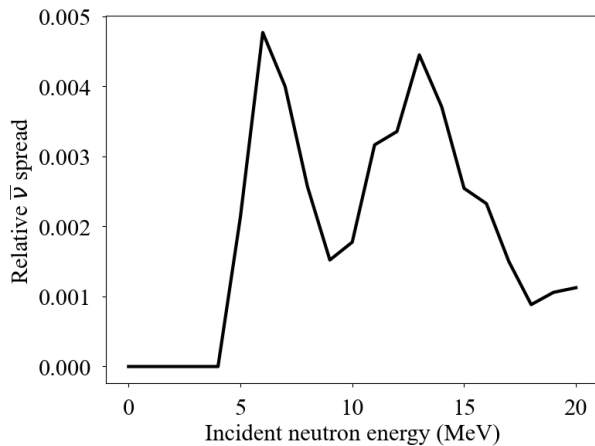


**Figure 5.** Relative spread in  $\bar{\nu}$  for  $^{239}\text{Pu}(n,f)$  as a function of incident neutron energy for the calculations in Fig. 4.

## 4 Summary and Outlook

A detailed analysis was conducted to evaluate the uncertainties of the fission cross section for selected  $^{235}\text{U}$  experimental data within the Neutron Data Standard database using the template of expected measurement uncertainties. The subsequent comparison of sampled  $^{239}\text{Pu}$  fission cross sections in CoH allowed us to investigate the change in prompt fission observables in CGMF, particularly to the average prompt neutron multiplicity,  $\bar{\nu}$ . This investigation showed the absence of a strong correlation between the spreads in multi-chance fission probabilities and  $\bar{\nu}$  when only the multi-chance fission probabilities were varied. Moving forward, we will continue to investigate the impact of the sampled multi-chance probabilities on other prompt fission observables, along with whether any of these conclusions change when other input into CGMF are sampled simultaneously.

Moreover, we would like to initiate a potential collaboration with the Neutron Data Standards committee to facilitate the update of fission cross-section uncertainties for  $^{235}\text{U}$  experimental data, mirroring the successful update done for the  $^{239}\text{Pu}$  experimental data used in this project.

## 5 Acknowledgement

Research reported in this publication was supported by the U.S. Department of Energy LDRD program at Los Alamos National

Laboratory and the ASC program. Los Alamos National Laboratory is operated by Triad National Security, LLC, for the National Nuclear Security Administration of the US Department of Energy under Contract No. 89233218CNA000001.

## References

- [1] A.D. Carlson et al., Evaluation of the Neutron Data Standards, Nucl. Data Sheets **148**, 143 (2018). <https://doi.org/10.1016/j.nds.2018.02.002>
- [2] D. Neudecker et al., Applying a template of expected uncertainties to updating  $^{239}\text{Pu}(n, f)$  cross-section covariances in the neutron data standards database, Nucl. Data Sheets **163**, 228 (2020). <https://doi.org/10.1016/j.nds.2019.12.005>
- [3] D. Neudecker, ARIADNE – a program estimating covariances in detail for neutron experiments, EPJ Nuclear Sci. Technol. **4**, 34 (2018). <https://doi.org/10.1051/epjn/2018012>
- [4] D. Neudecker, Templates of expected measurement uncertainties, EPJ Nuclear Sci. Technol. **9**, 35 (2023). <https://doi.org/10.1051/epjn/2023014>
- [5] T. Kawano, Unified description of the coupled-channels and statistical Hauser-Feshbach nuclear reaction theories for low energy neutron incident reactions, Eur. Phys. J. A **57**, 16 (2021). <https://doi.org/10.1140/epja/s10050-020-00311-9>
- [6] P. Talou et al., Fission fragment decay simulations with the CGMF code, Comp. Phys. Comm. **269**, 108087 (2021). <https://doi.org/10.1016/j.cpc.2021.108087>
- [7] V.V. Zerkin, B. Pritychenko, The Experimental Nuclear Reaction Data (EXFOR): Extended Computer Database and Web Retrieval System, Nucl. Instrum. Methods Phys. Res. A **888**, 31 (2018). <https://doi.org/10.1016/j.nima.2018.01.045>
- [8] B. Whewell et al., Evaluating  $^{239}\text{Pu}(n,f)$  cross sections via machine learning using experimental data, covariances, and measurement features, Nucl. Instrum. Methods Phys. Res. A **978**, 164305 (2020). <https://doi.org/10.1016/j.nima.2020.164305>
- [9] N. N. Buleeva, et al., Activation-measured radiative neutron-capture cross sections for  $^{236}\text{U}$ ,  $^{238}\text{U}$ , and  $^{237}\text{Np}$ , Soviet Atomic Energy **65**, 920 (1988). <https://doi.org/10.1007/BF01121252>